
UNIVERSAL NUCLEATION BEHAVIOR OF SHEARED SYSTEMS

A PREPRINT

 **Amrita Goswami**

Department of Chemical Engineering
Indian Institute of Technology Kanpur
amritag@iitk.ac.in

Indranil Saha Dalal*

Department of Chemical Engineering
Indian Institute of Technology Kanpur
indrasd@iitk.ac.in

 **Jayant K. Singh***

Department of Chemical Engineering
Indian Institute of Technology Kanpur
jayantks@iitk.ac.in

December 11, 2021

ABSTRACT

Using molecular simulations and a modified Classical Nucleation Theory, we study the nucleation, under flow, of a variety of liquids: different water models, Lennard-Jones and hard sphere colloids. Our approach enables us to analyze a wide range of shear rates inaccessible to brute-force simulations. Our results reveal that the variation of the nucleation rate with shear is universal. A simplified version of the theory successfully captures the non-monotonic temperature dependence of the nucleation behavior, which is shown to originate from the violation of the Stokes-Einstein relation.

Keywords rare-event, nucleation, shear, seeding, Classical Nucleation Theory

1 Introduction

The nucleation of quiescent systems, at molecular scales, is of major interest and has been the focus of intense research [1]. However, in nature and in practice, static fluids are rarely involved; realistic systems almost always exist in a state of flux. The study of the effects of shear on nucleation is a burgeoning field, with far-reaching implications for industry and several branches of science. Despite investigations in this direction, the literature is rife with controversial results. Some studies indicate that the presence of shear inhibits the nucleation rate [2, 3], while others assert that the nucleation rate is enhanced by shear [4–10]. A non-monotonic dependence of the induction times for nucleation has also been reported in experiments [11, 12].

The homogeneous nucleation of the sheared Ising model [13], colloidal models [14, 15], hard spheres (HS) [16–18], glassy systems [19, 20], a binary-alloy [21], and more recently mW water under shear [22, 23], has been studied using theory and simulations. Water is a highly anomalous liquid exhibiting several anomalies in the supercooled regime [24], but efforts have not been made to distinguish the nature of the shear-dependent nucleation behavior of water, or to generalize shared traits. However, existing literature implies that the nucleation rate for liquids, including water, is non-monotonic with shear [14–23].

In this work, we generalize the phenomenon of shear-induced nucleation by revealing the underlying universality of the same. Recently we formulated a Classical Nucleation Theory (CNT), extended to explicitly incorporate shear [23]. Here, we show the generality of this approach (henceforth referred to as 'shear-CNT'), using it to explain the effects of shear on various systems: the rigid water models TIP4P/2005 [25], TIP4P/Ice [26], the coarse-grained mW water model [27], the Lennard-Jones (LJ) fluid [28], and a HS colloid. We examine, in detail, the dual effects of temperature and shear on the nucleation rates for water and LJ fluid, explore the provenance of anomalies, and highlight the universality in the nucleation behavior.

*Corresponding Author

2 Theory and Methods

The free energy of a crystal nucleus in a bulk homogeneous nucleating system, under the effect of a simple volume-preserving shear $\dot{\gamma}$, is given by [17]:

$$F(R) = -\frac{4}{3}\pi R^3 \frac{|\Delta\mu_0|}{v'} + 4\pi R^2 \sigma_0 \left[1 + \frac{7}{24}(\tau\dot{\gamma})^2 \right] + \frac{1}{2}G(\tau\dot{\gamma})^2 \frac{4}{3}\pi R^3, \quad (1)$$

where $F(R)$ is the free energy of formation of a cluster of radius R , $|\Delta\mu_0|$ is the chemical potential difference between the thermodynamically stable crystal phase and the metastable liquid phase when no shear is applied, σ_0 is the surface tension or the interfacial free energy of the nucleus at zero shear, v' is the volume of one molecule in the crystal phase, G is the shear modulus of the nucleus, and τ is a characteristic time defined as $\tau = \frac{\eta}{G}$, where η is the fluid viscosity.

Homogeneous nucleation is an activated process, exhibiting a maximum in the free energy at a critical nucleus size N^* . The height of the free energy barrier for nucleation, corresponding to this critical nucleus size N^* , is obtained from

$$F(N^*) = \frac{N_0^* |\Delta\mu_0|}{2} \frac{[1 + \frac{7}{24}(\tau\dot{\gamma})^2]^3}{\left[1 - \frac{v'G}{2|\Delta\mu_0|}(\tau\dot{\gamma})^2\right]^2}, \quad (2)$$

where $N_0^* = \frac{32\pi\sigma_0^3 v'^2}{3|\Delta\mu_0|^3}$ is the critical nucleus size at zero shear.

The steady-state nucleation rate, J , can be estimated using the following familiar CNT-based expression [23]:

$$J = \rho_l Z f^+ e^{-\frac{F(N^*)}{k_B T}}, \quad (3)$$

where the nucleation rate J is the current or flux across the free energy barrier, in the cluster-size space and is in units of the number of nucleation events per unit volume per unit time, f^+ is the rate of attachment of particles to the critical cluster, ρ_l is the number density of the supercooled liquid, and Z is the Zeldovich factor. Z captures the probability of multiple re-crossings of the energy barrier[29].

The expression for the shear rate-dependent attachment rate f^+ is given by [23]:

$$f^+ = \frac{24D_l}{\lambda^2} (N^*)^{\frac{2}{3}} \left[1 + \frac{7}{24}(\tau\dot{\gamma})^2 \right], \quad (4)$$

where D_l is the two-dimensional diffusion coefficient of the supercooled liquid phase for a particular shear rate and temperature T , and λ is the atomic ‘jump length’, estimated to be about one molecule diameter.

It has been shown earlier that the diffusion coefficient varies linearly with shear rates, at a constant temperature, for the mW model [23]:

$$D_l = D_0 + c\dot{\gamma}, \quad (5)$$

where D_0 is the diffusion coefficient when the shear rate is zero, and c is a fitting parameter with units of squared length. We observe that Eq. (5) holds true for TIP4P/2005, TIP4P/Ice, mW and LJ. We have estimated c for these systems by fitting D_l , from out non-equilibrium molecular dynamics (NEMD) simulations, to Eq. (5). Such a linear behavior is predicted for a suspension of particles, which also provide the following estimate for c [30, 31]:

$$c = K_c a^2 \phi, \quad (6)$$

where a is the particle diameter, ϕ is the volume fraction, and K_c is a constant. We have used a value of $K_c = 0.4$, which has been successfully used for suspensions [30] and blood [31]. In this letter, for hard-sphere colloids, we use Eq (6) to estimate the value of c . D_0 is calculated using the Stokes-Einstein relation, given by $D_0 = (\rho_l)^{\frac{1}{3}} \frac{k_B T}{6\eta}$, modified for hard spheres [32].

We note that the shear rates considered in this study are low enough to safely assume that the fluids exhibit Newtonian behavior. Further, we assume that the shear modulus G of the nuclei is isotropic, which may not be strictly true for ice. However, the variations in G for both hexagonal ice and amorphous ice are within the range of 3 – 4.5 *GPa* [33–35], which does not significantly impact the calculated nucleation rates [23].

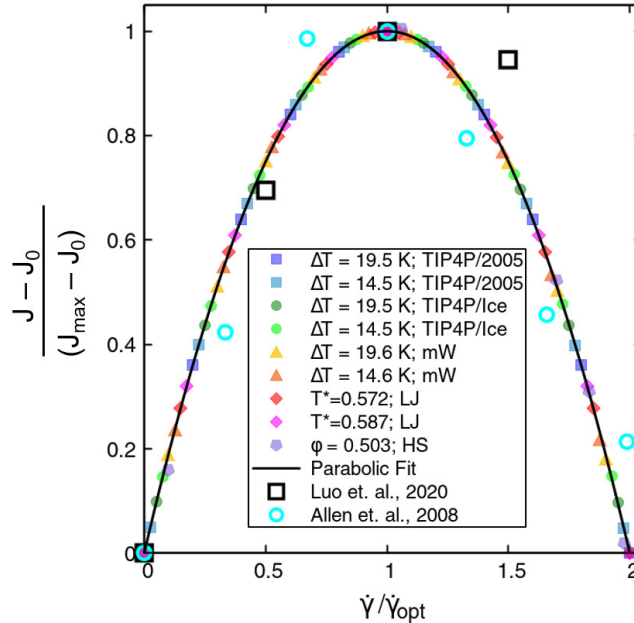


Figure 1: Variation of the normalized nucleation rate with the normalized shear rate, $\dot{\gamma}/\dot{\gamma}_{opt}$ at selected metastabilities, plotted alongside the corresponding parabolic fit. Eq. (7) has been denoted by a solid black line, and filled markers symbolize the nucleation rates calculated using shear-CNT for various systems and metastabilities. Black open squares show the data for the mW model estimated by Luo et. al. [22], for a supercooling of 67.6 K, using brute-force NEMD to calculate and fit to the induction times [37]. Open turquoise circles depict the data for a sheared two-dimensional Ising model, obtained using Forward-Flux Sampling [38], by Allen et. al. [13]

3 Results and Discussion

The shear-CNT formulation predicts that the nucleation rate J has a non-monotonic nature with respect to the shear rate, owing to competing energetic and kinetic effects. Eq. (2) shows that the free energy barrier will rise with increasing shear rates. Eq. (4) indicates that f^+ will increase, due to the increase in both D_l and N^* . The net effect is that of a maximum in J (Eq. (3)) at some particular shear rate.

To analyze the non-monotonicity, we introduce a min-max normalized [36] nucleation rate, $\frac{J-J_0}{J_{max}-J_0}$, defined with respect to J_0 , the nucleation rate at zero shear, and J_{max} , the highest nucleation rate observed at a particular temperature [23]. The optimal shear rate, $\dot{\gamma}_{opt}$, is defined as the shear rate for which $\frac{J-J_0}{J_{max}-J_0}$ is maximized.

We observe that, for all the systems studied in this work, parabolic fits approximate the nucleation rate behavior with excellent agreement. A parabolic law, with respect to the dimensionless shear $\frac{\dot{\gamma}}{\dot{\gamma}_{opt}}$, of the following form can describe the nucleation behavior at a particular temperature T and supercooling ΔT :

$$\frac{J - J_0}{J_{max} - J_0} = 1 - \left(\frac{\dot{\gamma}}{\dot{\gamma}_{opt}} - 1 \right)^2, \quad (7)$$

The vertex of this parabola is at unity. We recover a family of parabolas with vertices at $\dot{\gamma}_{opt}$, at every temperature, if $\frac{J-J_0}{J_{max}-J_0}$ is plotted against $\dot{\gamma}$.

Figure 1 depicts the universality in the normalized nucleation rate, generated by the superposition of available data for the water models, LJ fluid and hard spheres. These include our results, as well as those of earlier studies by other groups [13, 22]. We infer the existence of a single maximum nucleation rate, at any given metastability, for every system. For shear rates higher than $\dot{\gamma}_{opt}$, the nucleation rate decreases. Despite the complex interactions of shear-dependent terms in Eq. (3), the simple functional form of Eq. (7) works well for all systems. These results indicate that this behavior is fundamental to Newtonian fluids.

A previous study on the mW model suggests that the shear-dependent nucleation rates have a non-linear dependence on the temperature [23]. This could arise from the inclusion of several temperature-dependent parameters in the expression

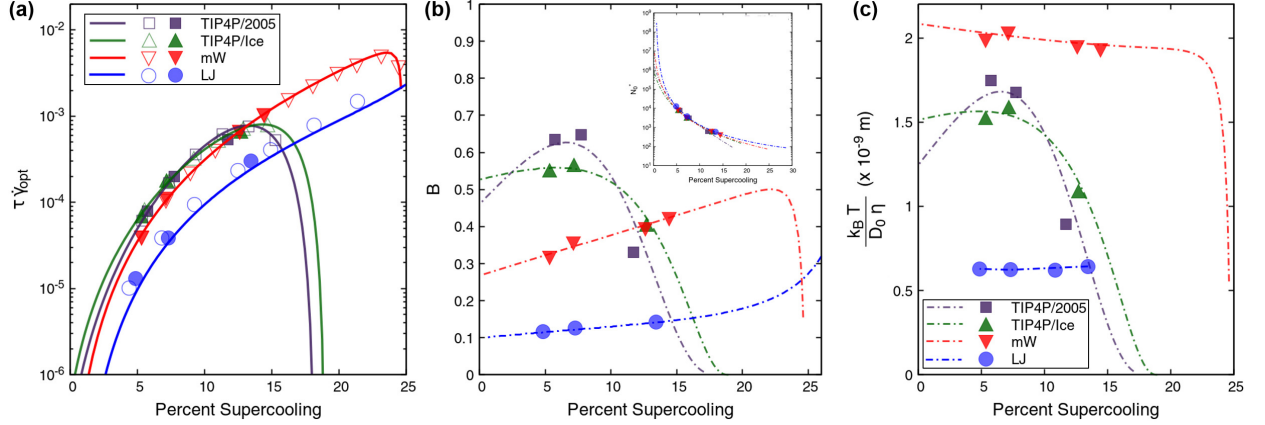


Figure 2: (a) Dependence of $\tau\dot{\gamma}_{opt}$ on the percent supercooling, $\frac{T_m - T}{T_m} \times 100\%$, for TIP4P/2005, TIP4P/Ice, mW and LJ. Filled and open markers represent values calculated using shear-CNT, with input data calculated from simulations and with approximated inputs, respectively. The solid lines denote $\tau\dot{\gamma}_{opt}$ estimated using the simplified theory, Eq. (9). (b) Variation of $B = \left(\frac{k_B T c}{D_0 \eta v'}\right)$ with the percent supercooling. The inset shows N_0^* plotted against the percent supercooling. (c) Test of the Stokes-Einstein (SE) relation, according to which $\frac{k_B T}{D_0 \eta}$ should be constant. SE relation is clearly violated for the water models for the supercoolings considered. Data for which the values of η , D_0 , c and v' were calculated using simulation data are denoted by filled markers, and dashed lines show values calculated using approximations.

for the nucleation rate (Eq. (3)). Scrutiny of Eq. (1), Eq. (2) and Eq. (4) reveals the recurring dimensionless group $\tau\dot{\gamma}$. The temperature dependence of the nucleation behavior under shear is embodied by the dimensionless product, $\tau\dot{\gamma}_{opt}$, where $\dot{\gamma}_{opt}$ depends on the temperature as well as the nature of the system. However, the transcendental nature of the nucleation rate expression prevents us from directly solving an analytical expression for $\tau\dot{\gamma}_{opt}$.

In order to further simplify the governing equations of the shear-CNT formalism and obtain a relation for $\tau\dot{\gamma}_{opt}$, we examine the order of magnitudes for the various parameters in the equations involved. For water, LJ and HS, the shape factor is ≈ 1 for the highest shear rates considered. For $\dot{\gamma} < \frac{1}{\eta} \left(\frac{2G|\Delta\mu_0|}{v'}\right)^{\frac{1}{2}}$, we can use a binomial expansion for the denominator in Eq. (2). Subsequently expanding the exponential in Eq. (3), we finally obtain a simplified expression for J :

$$J = J_0 \left(1 + \frac{c}{D_0}\right) \left[1 - \frac{N_0^* v' G}{2k_B T} (\tau\dot{\gamma})^2\right], \quad (8)$$

where J_0 is the nucleation rate when the shear rate is zero. We note that, although Eq. (8) is cubic in $\dot{\gamma}$, there exists only one positive root $\dot{\gamma}_{opt}$. This is reflected by the existence of a single maximum in the master curve for the normalized nucleation rate, shown in Fig. 1.

As the magnitude of the dimensionless term $\frac{6c^2 G k_B T}{N_0^* v' (D_0 \eta)^2}$ is one and two orders of magnitude lower than unity for the water models and LJ, respectively, we obtain the following relation for $\tau\dot{\gamma}_{opt}$:

$$\tau\dot{\gamma}_{opt} = \left(\frac{k_B T c}{D_0 \eta v'}\right) \times \frac{1}{N_0^*}, \quad (9)$$

where we define $B = \left(\frac{k_B T c}{D_0 \eta v'}\right)$, which is a dimensionless group related to the transport properties. N_0^* is dependent on the thermodynamic properties. η and D_0 are approximated by power law fits. Second-order polynomials suffice to approximate the densities [39]. Linear fits to σ_0 [39], $|\Delta\mu_0|$, c , are used to obtain the predicted values. To compare the behavior of the water models and LJ fluid, we define the percent supercooling with respect to the melting point, T_m , for each model.

Figure 2(a) shows the variation in $\tau\dot{\gamma}_{opt}$ with percent supercooling for the water models and LJ. The simplified Eq. (9) performs well for the models considered (denoted by lines in Fig. 2). $\tau\dot{\gamma}_{opt}$ exhibits a single maximum for every water model. In particular, the rigid water models show nearly identical behavior. We also note that every system shows monotonic increase in the limit of 10% supercooling. However, the $\tau\dot{\gamma}_{opt}$ curve for LJ shows a qualitatively different trend compared to the water models for higher supercooling.

Figure 2(b) depicts the dependence of the dimensionless group B on the percent supercooling. The non-monotonic behavior of B for the water models closely mirrors that of $\tau\dot{\gamma}_{opt}$ in Fig. 2(a). Concomitantly, we attribute the trend in $\tau\dot{\gamma}_{opt}$ for LJ to the monotonic behavior of B . The inset of Fig 2(b) shows a nearly universal trend of N_0^* with percent supercooling.

Furthermore, our analysis shows that the origin of the divergent trends in B (Fig. 2(b)) lies in the Stokes-Einstein (SE) relation. Anomalous transport properties of supercooled liquids are often characterized by SE violation [40–48]. According to the SE relation, the following expression holds true at all temperatures [49, 50]:

$$D_0 \propto \frac{k_B T}{\eta}, \quad (10)$$

which implies that, if the SE relation is valid, the term $\frac{k_B T}{D_0 \eta}$ is constant.

Figure 2(c) depicts the variation of $\frac{k_B T}{D_0 \eta}$ with percent supercooling. The SE relation breaks down spectacularly for supercooled water [48, 51–53], as shown by maxima in the $\frac{k_B T}{D_0 \eta}$ curves for TIP4P/2005, TIP4P/Ice and mW. These are directly reflected by the maxima of B and $\tau\dot{\gamma}_{opt}$ for the water models. In contrast, $\frac{k_B T}{D_0 \eta}$ is relatively constant for LJ (Fig. 2(c)), which suggests that the SE relation is preserved, in the case of the LJ fluid, for the supercoolings considered in this work. We surmise that the temperature dependence of the nucleation behavior is strongly linked to the violation or preservation of the SE relation, and thus depends solely on the behavior of flow properties. The decoupling of D_0 and η , typified by the SE violation, is thought to originate from spatial heterogeneities in the dynamics of strongly supercooled glass-forming liquids [40, 44, 46, 48, 53–55].

4 Conclusions

In conclusion, we have reported the effects of shear on the nucleation rates at different temperatures, for the TIP4P/2005, TIP4P/Ice, mW water models, LJ fluid and HS colloids. Nucleation events at low and moderate supercoolings are notoriously difficult to simulate, and such extensive calculations are virtually intractable using brute-force molecular dynamics. By employing the shear-CNT formalism, based on modified CNT equations, we were able to obtain nucleation rate curves for several metastable conditions.

In accordance with previous simulation results for colloids, glassy systems, the Ising model, and mW water [13, 16, 17, 22, 23], we confirmed that the nucleation rate curves exhibit non-monotonic behavior with shear, at a particular supercooling. We generated a "universal" master curve for the normalized nucleation rate $\frac{J-J_0}{J_{max}-J_0}$ with $\dot{\gamma}/\dot{\gamma}_{opt}$. Despite the complicated dependence of shear in the transcendental equation for the nucleation rate, parabolic fits yield excellent agreement to the nucleation rate curves and are valid for every system considered in this work. We infer that the existence of a maximum in the nucleation rate with shear is a universal property of systems that obey CNT.

We systematically investigated the temperature dependence of the nucleation rate curves for TIP4P/2005, TIP4P/Ice, mW and LJ by examining the behavior of the dimensionless group $\tau\dot{\gamma}_{opt}$. To this end, we derived a simplified theory describing the governing equations of shear-CNT. An approximate relation for $\tau\dot{\gamma}_{opt}$ was obtained, expressed as a product of two dimensionless groups: B , which is related to transport properties, and the thermodynamic quantity $1/N_0^*$. The analysis reveals that the behavior of $\tau\dot{\gamma}_{opt}$ is solely determined by the nature of B . The anomalous temperature dependence of the nucleation behavior of water originates from the SE violation. We discovered that universal behavior is recovered for N_0^* , for every system.

Thus, we have uncovered underlying commonalities and determined the origin of anomalies in the nucleation behavior for several supercooled molecular systems under shear. Our results provide insight into the previously unexplored, intriguingly complex interplay of temperature and shear, affecting the nucleation rate.

5 Acknowledgements

This work was supported by the Science and Engineering Research Board (sanction number STR/2019/000090 and CRG/2019/001325). Computational resources were provided by the HPC cluster of the Computer Center (CC), Indian Institute of Technology Kanpur.

References

1. Sosso, G. C. *et al.* Crystal Nucleation in Liquids: Open Questions and Future Challenges in Molecular Dynamics Simulations. *Chemical Reviews* **116**, 7078–7116 (May 2016).
2. Blaak, R., Auer, S., Frenkel, D. & Löwen, H. Crystal Nucleation of Colloidal Suspensions under Shear. *Physical Review Letters* **93** (Aug. 2004).
3. Blaak, R., Auer, S., Frenkel, D. & Löwen, H. Homogeneous nucleation of colloidal melts under the influence of shearing fields. *Journal of Physics: Condensed Matter* **16**, S3873–S3884 (Sept. 2004).
4. Mokshin, A. V. & Barrat, J.-L. Shear induced structural ordering of a model metallic glass. *The Journal of Chemical Physics* **130**, 034502 (Jan. 2009).
5. Graham, R. S. & Olmsted, P. D. Coarse-Grained Simulations of Flow-Induced Nucleation in Semicrystalline Polymers. *Physical Review Letters* **103** (Sept. 2009).
6. Radu, M. & Schilling, T. Solvent hydrodynamics speed up crystal nucleation in suspensions of hard spheres. *EPL (Europhysics Letters)* **105**, 26001 (Jan. 2014).
7. Forsyth, C. *et al.* Influence of Controlled Fluid Shear on Nucleation Rates in Glycine Aqueous Solutions. *Crystal Growth & Design* **15**, 94–102 (Nov. 2014).
8. Shao, Z. *et al.* Shear-accelerated crystallization in a supercooled atomic liquid. *Physical Review E* **91** (Feb. 2015).
9. Ruiz-Franco, J. *et al.* Crystal-to-Crystal Transition of Ultrasoft Colloids under Shear. *Physical Review Letters* **120** (Feb. 2018).
10. Stroobants, S. *et al.* Influence of Shear on Protein Crystallization under Constant Shear Conditions. *Crystal Growth & Design* **20**, 1876–1883 (Feb. 2020).
11. Holmqvist, P., Lettinga, M. P., Buitenhuis, J. & Dhont, J. K. G. Crystallization Kinetics of Colloidal Spheres under Stationary Shear Flow. *Langmuir* **21**, 10976–10982 (Nov. 2005).
12. Liu, J. & Rasmuson, Å. C. Influence of Agitation and Fluid Shear on Primary Nucleation in Solution. *Crystal Growth & Design* **13**, 4385–4394 (Sept. 2013).
13. Allen, R. J., Valeriani, C., Tănase-Nicola, S., ten Wolde, P. R. & Frenkel, D. Homogeneous nucleation under shear in a two-dimensional Ising model: Cluster growth, coalescence, and breakup. *The Journal of Chemical Physics* **129**, 134704 (Oct. 2008).
14. Cerdà, J. J., Sintes, T., Holm, C., Sorensen, C. M. & Chakrabarti, A. Shear effects on crystal nucleation in colloidal suspensions. *Physical Review E* **78** (Sept. 2008).
15. Lander, B., Seifert, U. & Speck, T. Crystallization in a sheared colloidal suspension. *The Journal of Chemical Physics* **138**, 224907 (June 2013).
16. Richard, D. & Speck, T. The role of shear in crystallization kinetics: From suppression to enhancement. *Scientific Reports* **5** (Sept. 2015).
17. Mura, F. & Zaccone, A. Effects of shear flow on phase nucleation and crystallization. *Physical Review E* **93** (Apr. 2016).
18. Richard, D. & Speck, T. Classical nucleation theory for the crystallization kinetics in sheared liquids. *Physical Review E* **99** (June 2019).
19. Mokshin, A. V. & Barrat, J.-L. Crystal nucleation and cluster-growth kinetics in a model glass under shear. *Physical Review E* **82** (Aug. 2010).
20. Mokshin, A. V., Galimzyanov, B. N. & Barrat, J.-L. Extension of classical nucleation theory for uniformly sheared systems. *Physical Review E* **87** (June 2013).
21. Peng, H. L., Herlach, D. M. & Voigtmann, T. Crystal growth in fluid flow: Nonlinear response effects. *Physical Review Materials* **1** (Aug. 2017).
22. Luo, S., Wang, J. & Li, Z. Homogeneous Ice Nucleation Under Shear. *The Journal of Physical Chemistry B* **124**, 3701–3708 (Mar. 2020).
23. Goswami, A., Dalal, I. S. & Singh, J. K. Seeding method for ice nucleation under shear. *The Journal of Chemical Physics* **153**, 094502 (Sept. 2020).

24. Pettersson, L. G. M., Henschman, R. H. & Nilsson, A. Water—The Most Anomalous Liquid. *Chemical Reviews* **116**, 7459–7462 (July 2016).
25. Abascal, J. L. F. & Vega, C. A general purpose model for the condensed phases of water: TIP4P/2005. *The Journal of Chemical Physics* **123**, 234505 (Dec. 2005).
26. Abascal, J. L. F., Sanz, E., Fernández, R. G. & Vega, C. A potential model for the study of ices and amorphous water: TIP4P/Ice. *The Journal of Chemical Physics* **122**, 234511 (June 2005).
27. Molinero, V. & Moore, E. B. Water Modeled As an Intermediate Element between Carbon and Silicon†. *The Journal of Physical Chemistry B* **113**, 4008–4016 (Apr. 2009).
28. Broughton, J. & Gilmer, G. Surface free energy and stress of a Lennard-Jones crystal. *Acta Metallurgica* **31**, 845–851 (June 1983).
29. Pan, A. C. & Chandler, D. Dynamics of Nucleation in the Ising Model†. *The Journal of Physical Chemistry B* **108**, 19681–19686 (Dec. 2004).
30. Siqueira, I., Rebouças, R. & Carvalho, M. Migration and alignment in the flow of elongated particle suspensions through a converging-diverging channel. *Journal of Non-Newtonian Fluid Mechanics* **243**, 56–63 (May 2017).
31. Chandran, K., Dalal, I. S., Tatsumi, K. & Muralidhar, K. Numerical simulation of blood flow modeled as a fluid-particulate mixture. *Journal of Non-Newtonian Fluid Mechanics* **285**, 104383 (Nov. 2020).
32. Ohtori, N., Uchiyama, H. & Ishii, Y. The Stokes-Einstein relation for simple fluids: From hard-sphere to Lennard-Jones via WCA potentials. *The Journal of Chemical Physics* **149**, 214501 (Dec. 2018).
33. Loerting, T. & Giovambattista, N. Amorphous ices: experiments and numerical simulations. *Journal of Physics: Condensed Matter* **18**, R919–R977 (Nov. 2006).
34. Cao, P. *et al.* Mechanical properties of bi- and poly-crystalline ice. *AIP Advances* **8**, 125108 (Dec. 2018).
35. Moreira, P. A. F. P., de Aguiar Veiga, R. G. & de Koning, M. Elastic constants of ice Ih as described by semi-empirical water models. *The Journal of Chemical Physics* **150**, 044503 (Jan. 2019).
36. Freedman, D., Pisani, R. & Purves, R. *Statistics* 720 pp. ISBN: 0393930432 (Norton & Company, May 1, 2018).
37. Fitzner, M., Sosso, G. C., Cox, S. J. & Michaelides, A. The Many Faces of Heterogeneous Ice Nucleation: Interplay Between Surface Morphology and Hydrophobicity. *Journal of the American Chemical Society* **137**, 13658–13669 (Oct. 2015).
38. Allen, R. J., Warren, P. B. & ten Wolde, P. R. Sampling Rare Switching Events in Biochemical Networks. *Physical Review Letters* **94** (Jan. 2005).
39. Espinosa, J. R., Vega, C., Valeriani, C. & Sanz, E. Seeding approach to crystal nucleation. *The Journal of Chemical Physics* **144**, 034501 (Jan. 2016).
40. Hodgdon, J. A. & Stillinger, F. H. Stokes-Einstein violation in glass-forming liquids. *Physical Review E* **48**, 207–213 (July 1993).
41. Stillinger, F. H. A Topographic View of Supercooled Liquids and Glass Formation. *Science* **267**, 1935–1939 (Mar. 1995).
42. Tarjus, G. & Kivelson, D. Breakdown of the Stokes–Einstein relation in supercooled liquids. *The Journal of Chemical Physics* **103**, 3071–3073 (Aug. 1995).
43. Cicerone, M. T. & Ediger, M. D. Relaxation of spatially heterogeneous dynamic domains in supercooled ortho-terphenyl. *The Journal of Chemical Physics* **103**, 5684–5692 (Oct. 1995).
44. Ediger, M. D. Spatially heterogeneous dynamics in supercooled liquids. *Annual Review of Physical Chemistry* **51**, 99–128 (Oct. 2000).
45. Shi, Z., Debenedetti, P. G. & Stillinger, F. H. Relaxation processes in liquids: Variations on a theme by Stokes and Einstein. *The Journal of Chemical Physics* **138**, 12A526 (Mar. 2013).
46. Sengupta, S., Karmakar, S., Dasgupta, C. & Sastry, S. Breakdown of the Stokes-Einstein relation in two, three, and four dimensions. *The Journal of Chemical Physics* **138**, 12A548 (Mar. 2013).
47. Henritzi, P., Bormuth, A., Klameth, F. & Vogel, M. A molecular dynamics simulations study on the relations between dynamical heterogeneity, structural relaxation, and self-diffusion in viscous liquids. *The Journal of Chemical Physics* **143**, 164502 (Oct. 2015).
48. Kawasaki, T. & Kim, K. Identifying time scales for violation/preservation of Stokes-Einstein relation in supercooled water. *Science Advances* **3**, e1700399 (Aug. 2017).
49. Sutherland, W. LXXV. A dynamical theory of diffusion for non-electrolytes and the molecular mass of albumin. *The London, Edinburgh, and Dublin Philosophical Magazine and Journal of Science* **9**, 781–785 (June 1905).
50. Hynes, J. T. Statistical Mechanics of Molecular Motion in Dense Fluids. *Annual Review of Physical Chemistry* **28**, 301–321 (Oct. 1977).

51. Chen, S.-H. *et al.* The violation of the Stokes-Einstein relation in supercooled water. *Proceedings of the National Academy of Sciences* **103**, 12974–12978 (Aug. 2006).
52. Xu, L. *et al.* Appearance of a fractional Stokes–Einstein relation in water and a structural interpretation of its onset. *Nature Physics* **5**, 565–569 (July 2009).
53. Kawasaki, T. & Kim, K. Spurious violation of the Stokes–Einstein–Debye relation in supercooled water. *Scientific Reports* **9** (May 2019).
54. Stillinger, F. H. & Hodgdon, J. A. Translation-rotation paradox for diffusion in fragile glass-forming liquids. *Physical Review E* **50**, 2064–2068 (Sept. 1994).
55. Lombardo, T. G., Debenedetti, P. G. & Stillinger, F. H. Computational probes of molecular motion in the Lewis-Wahnström model for ortho-terphenyl. *The Journal of Chemical Physics* **125**, 174507 (Nov. 2006).